# Effective interaction for relativistic theory of nuclear structure

L. N. Savushkin,[1] S. Marcos,[2] M. L. Quelle,[3] P. Bernardos,[2] V. N. Fomenko,[4] and R. Niembro[2]
[1]*St. Petersburg Institute for Telecommunications, Department of Physics, 191065, St. Petersburg, Russia*
[2]*University of Cantabria, Faculty of Sciences, Department of Modern Physics, 39005, Santander, Spain*
[3]*University of Cantabria, Faculty of Sciences, Department of Applied Physics, 39005, Santander, Spain*
[4]*St. Petersburg Institute for Railway Engineering, Department of Mathematics, 197341, St. Petersburg, Russia*
(Received 27 March 1996)

An effective interaction for relativistic Hartree-Fock (HF) calculations of nuclear structure is constructed. It includes a nonlinear functional of the most simple general form taking into account interactions and self-interactions of isoscalar meson fields. The parameters are determined to reproduce Dirac-Brueckner HF nuclear matter results obtained from different types of one-boson-exchange potential (OBEP) fitting *NN* scattering data. The effective interaction is used then to calculate ground-state properties of finite nuclei. Results for some specific OBEP's (BM-B version) are in reasonable agreement with experiment. The symmetry energy coefficient, in particular, is well reproduced. It is found that the $\sigma^2\omega^2$ and $\omega^4$ components of the effective interaction play an important role. [S0556-2813(97)02401-1]

PACS number(s): 21.30.Fe, 21.10.−k, 21.60.Jz, 21.65.+f

## I. INTRODUCTION

In the past two decades steadily growing activity connected with investigating the role of relativity in nuclear physics has taken place [1–3], the theory of the nuclear ground state being of special interest. Several approaches for solving the problem for nuclear matter (NM) and finite nuclei have been developed. The first essential steps in this field have been connected with using either the relativistic Hartree method [4,5] or the relativistic Hartree-Fock (RHF) approach [6–8]. The theory involves several types of meson fields interacting with nucleons via coupling constants treated, some of them, as free parameters. These calculations can yield a good fitting for the ground-state properties of NM and finite nuclei (both spherical and deformed).

The next step, at the present stage already attempted, is to develop a Dirac theory of the Brueckner-Hartree-Fock type (DBHF), which would yield the nuclear bulk properties (binding energies, radii, etc.) starting from a meson-exchange nucleon-nucleon interaction that fits free-space *NN* scattering and deuteron data. In this case the nuclear saturation properties are derived entirely from the *NN* potential using no additional parameters. This approach looks appealing since it has stronger theoretical grounds. However, the relativistic Brueckner-Hartree-Fock (RBHF) description of a finite structure is a complicated problem, a much more complicated one than its nonrelativistic counterpart. Calculation of the relativistic Brueckner reaction matrices, carried out at present only for infinite NM, was started, developed, and realized in Refs. [9–11]. A detailed discussion of the relativistic Brueckner theory for NM can be found in Refs. [9–14].

As for finite nuclei, this program is carried out at present only within certain approximate methods developed by several theoretical groups [15–30]. Most of these methods introduce effective interactions that, being considered within Dirac mean-field or Dirac Hartree-Fock approximations, reproduce RBHF results of NM (the nucleon self-energy and binding energies). Effective interactions obtained in this way are utilized then to calculate properties of finite nuclei.

A main consequence of this method is that the meson-nucleon coupling constants can be density dependent, reflecting the genuine density dependence of the Dirac-Brueckner *NN G* matrix in the nuclear medium.

Recently, another effective $\sigma$-$\omega$ model, including nonlinear $\sigma$ and $\omega$ self-coupling terms, cubic and quartic self-interactions of the $\sigma$ field, and quartic self-interactions of the $\omega$ meson, was considered in Ref. [24]. The density dependence, in this case, comes through the effective meson masses. On the basis of that effective interaction, the properties of finite nuclei were calculated in the framework of the relativistic Hartree approximation.

In the present paper we also follow the philosophy of the effective Lagrangian and investigate the following model.

(1) All reasonable meson fields are taken into account, since it is hard to believe that a simple two meson model would account for all peculiar features of a Dirac-Brueckner method [28].

(2) The interactions of isoscalar meson fields (i.e., $\sigma\omega^2$ and $\sigma^2\omega^2$ terms) are also taken into consideration together with self-couplings of the $\sigma$ and $\omega$ mesons. Thus all interactions and self-interactions of the $\sigma$ and $\omega$ fields (in the most simple general form compatible with invariance considerations) are included. In our case, one of the key ingredients of the theory is the dressed meson masses [7,8].

(3) The RHF method is used both in the fitting procedure of the effective Lagrangian (to the DBHF results of NM with free *NN* forces) and in calculations of the ground-state properties of finite nuclei. The necessity to take into account the $\pi$ and $\rho$ mesons is one of the reasons to use the RHF approximation in the present investigation. The role of the isovector mesons in the RHF scheme (without self-interactions of mesons fields) has been studied earlier in Refs. [6,18,26, 29,30], while in Refs. [7,8] self-interactions were partially taken into account. In these investigations it was shown, in particular, that the Fock-exchange terms are not negligible and that important contributions from the isovector mesons

 © 1997 The American Physical Society

cannot be included in the mean-field approach.

In particular, the effect of the pion on the spin-orbit splittings was clearly demonstrated in Refs. [6,29]. In Ref. [29] it was shown that the spin-orbit splitting $\Delta_{LS}$ of the $1g_{9/2-7/2}$ neutron shell in $^{114}$Sn is decreased by almost a factor of 2 (without affecting the binding energy or charge radius significantly). The same was shown earlier to occur in $^{48}$Ca for the $1d_{5/2-3/2}$ proton spin-orbit splitting [6]. The pion is crucial to reproduce the drastic change of the spin-orbit splitting when going from $^{40}$Ca to $^{48}$Ca, the number of protons being the same in both nuclei.

It is known also [6,8,30] that RHF approach with $\pi$ and $\rho$ mesons reduces considerably the exaggerated shell effects obtained in the relativistic mean field (RMF) approximation for the density distributions inside nuclei.

All said above shows the general features of any RHF approach produced by $\pi$ and $\rho$ mesons.

The paper is organized as follows. In Sec. II the description of the model is given, the effective interaction is introduced, and a brief description of the RHF method for the model with nonlinear meson self-interaction and meson-meson interaction terms is made. In Sec. III the effective interaction is fitted, in the framework of RHF method, to NM observables obtained in the DBHF approach. The properties of finite nuclei are also calculated and compared with experiment. In Sec. IV the results are summarized and conclusions are drawn.

## II. GENERAL FORMALISM

The effective Lagrangian density $\mathcal{L}$ of our model is given by a sum of a free Lagrangian $\mathcal{L}_0(\varphi,\sigma,\omega,\rho,\pi,A)$, an interaction Lagrangian $\mathcal{L}_{\rm int}$(nucleon-meson), responsible for interaction of nucleons with different meson fields, and a nonlinear potential-energy functional $U_{\rm NL}$(meson-meson) taking into account meson self-interactions and meson-meson interactions of isoscalar meson fields:

$$\mathcal{L}=\mathcal{L}_0(\varphi,\sigma,\omega,\rho,\pi,A)+\mathcal{L}_{\rm int}(\text{nucleon-meson})-U_{\rm NL}(\text{meson-meson}). \tag{1}$$

The free Lagrangian density is given by

$$\mathcal{L}_0(\varphi,\sigma,\omega,\rho,\pi,A)=\overline{\varphi}(i\gamma_\mu\partial^\mu-M)\varphi-\tfrac{1}{2}m_\sigma^2\sigma^2+\tfrac{1}{2}(\partial_\mu\sigma\partial^\mu\sigma)+\tfrac{1}{2}m_\omega^2\omega_\mu\omega^\mu-\tfrac{1}{4}F_{\mu\nu}F^{\mu\nu}+\tfrac{1}{2}m_\rho^2\vec{\rho}_\mu\vec{\rho}^\mu-\tfrac{1}{4}\vec{G}_{\mu\nu}\vec{G}^{\mu\nu}$$
$$+\tfrac{1}{2}(\partial_\mu\vec{\pi}\cdot\partial^\mu\vec{\pi}-m_\pi^2\vec{\pi}^2)-\tfrac{1}{4}\vec{H}_{\mu\nu}\vec{H}^{\mu\nu}, \tag{2}$$

with

$$F_{\mu\nu}\equiv\partial_\nu\omega_\mu-\partial_\mu\omega_\nu,$$
$$\vec{G}_{\mu\nu}\equiv\partial_\nu\vec{\rho}_\mu-\partial_\mu\vec{\rho}_\nu,$$
$$H_{\mu\nu}\equiv\partial_\nu A_\mu-\partial_\mu A_\nu. \tag{3}$$

Here $M$, $m_\sigma$, $m_\omega$, $m_\rho$, and $m_\pi$ denote the bare masses of the nucleon and mesons, respectively, whereas $\varphi$, $\sigma$, $\omega_\mu$, $\vec{\rho}_\mu$, and $\vec{\pi}$ are the corresponding field operators (note that $\vec{\rho}_\mu$ and $\vec{\pi}$ are vectors in isospin space). Finally, $A_\mu$ is the electromagnetic field, realizing the Coulomb interaction between nucleons.

The meson-nucleon interaction Lagrangian is written as

$$\mathcal{L}_{\rm int}(\text{nucleon-meson})=-g_\sigma\overline{\varphi}\sigma\varphi-g_\omega\overline{\varphi}\gamma^\mu\omega_\mu\varphi-\frac{f_\omega}{2M}\,\overline{\varphi}\sigma^{\mu\nu}\partial_\mu\omega_\nu\varphi-g_\rho\overline{\varphi}\gamma^\mu\vec{\rho}_\mu\cdot\vec{\tau}\varphi-\frac{f_\rho}{2M}\,\overline{\varphi}\sigma^{\mu\nu}\partial_\mu\vec{\rho}_\nu\cdot\vec{\tau}\varphi$$
$$-e\overline{\varphi}\gamma^\mu\tfrac{1}{2}(1+\tau_3)A_\mu\varphi-\frac{f_\pi}{m_\pi}\,\overline{\varphi}\gamma_5\gamma^\mu\partial_\mu\vec{\pi}\cdot\vec{\tau}\varphi. \tag{4}$$

The isospin Pauli matrices are given by $\vec{\tau}$, $\tau_3$ being the third component of $\vec{\tau}$. The pion-nucleon interaction in Eq. (4) is chosen in a pseudovector form as in Refs. [6,7]. The quantities $g_i$ ($i=\sigma,\omega,\rho,\pi$) are the effective meson-nucleon coupling constants, while $f_\omega$ and $f_\rho$ are the isoscalar and isovector-tensor coupling constants and $e^2/4\pi=\frac{1}{137}$.

Finally, the potential-energy functional $U_{\rm NL}$(meson-meson) in Eq. (1) is taken in the form

$$U_{\rm NL}(\text{meson-meson})=U_{\rm NL}(\sigma,\omega)=\tfrac{1}{3}\overline{b}M(g_\sigma\sigma)^3+\tfrac{1}{4}\overline{c}(g_\sigma\sigma)^4+\overline{d}M(g_\sigma\sigma)(g_\omega^2\omega_\mu\omega^\mu)-\tfrac{1}{4}\overline{e}(g_\sigma\sigma)^2(g_\omega^2\omega_\mu\omega^\mu)-\tfrac{1}{4}\overline{f}(g_\omega^2\omega_\mu\omega^\mu)^2, \tag{5}$$

which is specified by five dimensionless parameters $\overline{b}$, $\overline{c}$, $\overline{d}$, $\overline{e}$, and $\overline{f}$. The form of $U_{\rm NL}(\sigma,\omega)$ given by Eq. (5) takes into account self-interactions of the isoscalar-scalar meson field (cubic and quartic terms in $\sigma$), quartic self-interactions of the isoscalar-vector meson field (the cubic self-interaction $\sim\omega^3$ is not introduced because of its parity), and terms which are responsible for interactions between isoscalar meson fields. Equation (5) is the most simple general form (compatible with relativistic invariance requirements) containing $\sigma$ and $\omega$ fields (see also Ref. [31]). Thus, introducing interactions and self-interactions between isoscalar meson fields (these interactions are represented diagrammatically in Fig. 1) is an im-

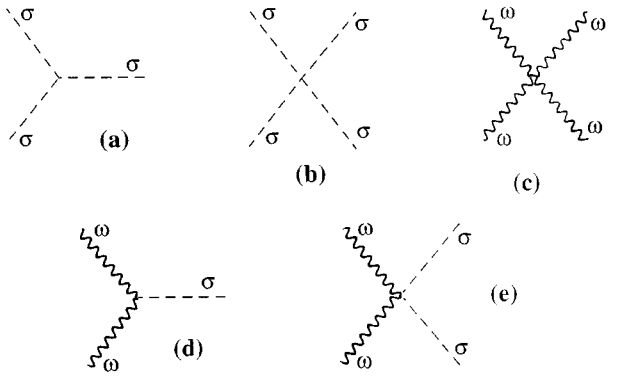


FIG. 1. Diagrammatic representation of interactions between isoscalar meson fields (the dashed line corresponds to the scalar meson while the wavy line corresponds to the $\omega$ field). Cases (a), (b), and (c) represent $\sigma^3$, $\sigma^4$, and $\omega^4$ self-interaction terms, respectively, whereas (d) and (e) represent $\sigma\omega^2$ and $\sigma^2\omega^2$ interaction terms, respectively.

portant feature of our approach. It should be emphasized that the inclusion of the functional $U_{\rm NL}$ into the general framework of relativistic description is a phenomenological procedure similar to that of considering the short-range two-body correlations. Let us notice also that separate components of the potential energy functional $U_{\rm NL}$ have been treated earlier by different authors.

Scalar self-interactions were introduced originally into the nuclear structure context in Refs. [32–36]. Extensive relativistic studies with cubic-plus-quartic scalar meson self-interactions have been carried out by the Hartree method both for spherical [4,5] and deformed nuclei [37]. In Ref. [38] a comparison of the relativistic mean field theory (with cubic-plus-quartic terms) and the Skyrme Hartree-Fock theory (for properties of nuclei and NM) was carried out. In Ref. [7], $\sigma^3+\sigma^4$ terms were successfully included into the framework of the relativistic Hartree-Fock theory of spherical nuclei.

Quartic self-coupling terms of the $\omega$ meson field were introduced into the relativistic theory in Ref. [39]. They were shown to be essential for obtaining a proper density dependence of the vector potential. The effective Lagrangian with $\omega^4$ self-interaction terms was utilized later in Refs. [24,40–42] in the framework of a relativistic mean-field theory for nuclear structure.

Finally, the inclusion of the $\sigma\omega^2$ and $\sigma^2\omega^2$ terms is motivated by investigations carried out in Ref. [8] and references therein.

The Euler-Lagrange equations for the various fields can be obtained from the Lagrangian density given by Eq. (2). For the nucleon field one has a Dirac equation

$$\Big\{ i\gamma^\mu\partial_\mu - M - g_\sigma\sigma - g_\omega\gamma^\mu\omega_\mu - \frac{f_\omega}{2M}\,\sigma^{\mu\nu}\partial_\mu\omega_\nu - g_\rho\gamma^\mu\vec{\rho}_\mu\cdot\vec{\tau} - \frac{f_\rho}{2M}\,\sigma^{\mu\nu}\partial_\mu\vec{\rho}_\nu\cdot\vec{\tau} - (e/2)\,\gamma^\mu(1+\tau_3)A_\mu - \frac{f_\pi}{m_\pi}\,\gamma_5\gamma^\mu\partial_\mu\vec{\pi}\cdot\vec{\tau}\Big\}\varphi(x) = 0, \tag{6a}$$

whereas for the meson and electromagnetic fields one has

$$(\Box + m_\sigma^{*2})\sigma = -g_\sigma\overline{\varphi}\varphi, \tag{6b}$$

$$(\Box + m_\omega^{*2})\omega_\nu = g_\omega\overline{\varphi}\gamma_\nu\varphi - \frac{f_\omega}{2M}\,\partial^\mu(\overline{\varphi}\sigma_{\mu\nu}\varphi), \tag{6c}$$

$$(\Box + m_\pi^2)\vec{\pi} = \frac{f_\pi}{m_\pi}\,\partial_\mu(\overline{\varphi}\gamma_5\gamma^\mu\vec{\tau}\varphi), \tag{6d}$$

$$(\Box + m_\rho^2)\vec{\rho}_\nu = g_\rho\overline{\varphi}\gamma_\nu\vec{\tau}\varphi - \frac{f_\rho}{2M}\,\partial^\mu(\overline{\varphi}\sigma_{\mu\nu}\vec{\tau}\varphi), \tag{6e}$$

$$\Box A_\nu = \frac{e}{2}\,\overline{\varphi}(1+\tau_3)\gamma_\nu\varphi. \tag{6f}$$

In Eqs. (6b) and (6c) $m_\sigma^*$ and $^*_\omega$ are the scalar and $\omega$-vector effective meson masses, respectively. They can be written in terms of the $\sigma$ and $\omega_\mu$ fields as

$$\begin{aligned} m_\sigma^{*2} &= m_\sigma^2 + \overline{b}g_\sigma^2 M(g_\sigma\sigma) + \overline{c}g_\sigma^2(g_\sigma\sigma)^2 + \overline{d}g_\sigma^2 M\,\frac{(g_\omega\omega_0)^2}{g_\sigma\sigma} \\ &\quad - \tfrac{1}{2}\overline{e}g_\sigma^2(g_\omega\omega_0)^2, \\ m_\omega^{*2} &= m_\omega^2 - 2\overline{d}Mg_\omega^2(g_\sigma\sigma) + \tfrac{1}{2}\overline{e}g_\omega^2(g_\sigma\sigma)^2 + \overline{f}g_\omega^2(g_\omega\omega_0)^2. \end{aligned} \tag{7}$$

To solve Eqs. (6) for $\sigma$ and $\omega_\mu$, we linearize them, replacing $\sigma$ and $\omega_0$ in $m_\sigma^{*2}$ and $m_\omega^{*2}$ by their ground-state expectation values. Then, the $\sigma$ and $\omega_\mu$ fields can be cast in the form

$$\sigma(x) = -g_\sigma\int S^{(\sigma)}(x,y)\,\overline{\varphi(y)}\,\varphi(y)\,d^4y, \tag{8a}$$

$$\omega_\mu(x) = g_\omega\int S^{(\omega)}(x,y)\,\overline{\varphi(y)}\,\gamma_\mu\varphi(y)\,d^4y, \tag{8b}$$

where $S^{(\sigma)}$ and $S^{(\omega)}$ are the $\sigma$ and $\omega$ meson propagators. They satisfy the equations

$$[\Box + m_\sigma^{*2}(r)]S^{(\sigma)}(x,y) = \delta(x-y), \tag{9a}$$

$$[\Box + m_\omega^{*2}(r)]S^{(\omega)}(x,y) = \delta(x-y). \tag{9b}$$

For the $\vec{\pi}$ and $\vec{\rho}_\mu$ fields one can write similar expressions to Eqs. (8a) and (8b) with the corresponding propagators $S^{(\pi)}$ and $S^{(\rho)}$. Note that the $\sigma$ and $\omega$ effective masses $m_\sigma^*$ and $m_\omega^*$ depend on $r$ and, consequently, $S^{(\sigma)}$ and $S^{(\omega)}$ do not have the simple Yukawa form as $S^{(\pi)}$ and $S^{(\rho)}$.

In the present paper we investigated an effective Lagrangian including interactions and self-interactions of isoscalar fields. The interactions of isovector fields formally can also be incorporated into the scheme of the present investigation. For example, one may take into account self-interactions of the $\rho$ meson field of the type $\mathcal{L}_{\rho\rho}^{\rm SI}\sim(g_\rho^2\vec{\rho}_\mu\cdot\vec{\rho}^\mu)^2$. However, since the $\rho$ meson contribution itself is small in comparison with that of the $\omega$ meson in the nuclear structure problems, we may hope that including $\mathcal{L}_{\rho\rho}^{\rm SI}$ will not influence essentially

the results obtained here. For this reason, this type of self-interactions is ignored at the present stage.

The nonlinear terms proportional to $\vec{\pi}^2\sigma^2$ and $\vec{\pi}^2\omega_\mu\omega^\mu$ (the strength of these interactions may be determined from chiral models) can be taken into account in the HF approximation as a density-dependent contribution to the pion mass and modifying the pion propagator in the same way as above for the $\sigma$ and $\omega_\mu$ fields [8]. However, it is known [1] that polarization effects induced by $\pi$ mesons in the nuclear medium also produce a density-dependent contribution to the pion mass. It can be shown that these two density-dependent contributions almost cancel each other. Just for this reason the pion mass in the nuclear medium is taken to be equal to its bare mass in the present investigation.

From $\mathcal{L}$ one can write down an equivalent Hamiltonian density as $H=H_0+H_1$, where $H_0$ is linear in the meson fields:

$$H_0=\overline{\varphi}(-i\vec{\gamma}\cdot\vec{\nabla}+M)\varphi+\tfrac{1}{2}\overline{\varphi}(g_\sigma\sigma+g_\omega\gamma^\mu\omega_\mu+\cdots)\varphi, \quad (10)$$

whereas $H_1$ contains only nonlinear terms like $\sigma^3$, $\sigma^4$, $\omega^4$, etc. The nonlinear character of $H_1$ makes the calculation of its exchange contribution to the energy rather complicated. Thus, as in $m_\sigma^{*2}$ and $m_\omega^{*2}$, we replace $\sigma$ and $\omega_\mu$ field operators in $H_1$ by their ground-state expectation values.

Using equivalent expressions to Eq. (8) for all the meson fields in the Dirac equation (deduced from $\mathcal{L}$) and $H_0$, we can write both of them in a form where only the nucleon fields $\varphi(x)$ are present. Then the Dirac equation can be obtained from $H_0$. Thus, in our approach, $H_1$ plays the role of a first order perturbation.

The nucleon field $\varphi(x)$ can be expanded on a complete set of stationary single-particle Dirac spinors $\{f_\alpha(\vec{x})e^{-iE_\alpha t}\}$. Assuming the tree approximation and the static limit for the meson fields, we obtain the Dirac equation for the spinor $f_\alpha(\vec{x})$:

$$[-i\vec{\alpha}\cdot\vec{\nabla}+\beta M+\beta\Sigma(\vec{x})]f_\alpha(\vec{x})=E_\alpha f_\alpha(\vec{x}). \quad (11)$$

This equation is formally identical to the corresponding one of Ref. [6] (where $U_{\rm NL}=0$); only the $\sigma$ and $\omega$ propagators are different (one can find more details in Ref. [7]).

To calculate the nucleon self-energy entering the Dirac equation, we can use the expressions developed in Ref. [6], replacing the Yukawa propagators of the $\sigma$ and $\omega$ mesons by the new ones [see Eqs. (9), for example]. In NM, $\Sigma$ is momentum dependent and can be written as [7]

$$\Sigma(p)=\Sigma_S(p)+\gamma_0\Sigma_0(p)+\vec{\gamma}\cdot\hat{p}\Sigma_V(p). \quad (12)$$

The scalar $\Sigma_S$, timelike $\Sigma_0$, and spacelike $\Sigma_V$ components of the self-energy are defined in Ref. [6]. In the present model, however, the free meson masses $m_\sigma$ and $m_\omega$ must be replaced by the respective effective masses $m_\sigma^*$ and $m_\omega^*$. One should have in mind also that the nonlinear part of the Hamiltonian $H_1$ should be taken into account when writing down the total energy of the system.

TABLE I. Saturation nuclear matter quantities fitted by our RHF approximation to reproduce DBHF NM results obtained from different types of OBEP's (BM-A, BM-B, DJM, and DJM-C).

| Type of OBEP | BM-A | BM-B | DJM | DJM-C |
|---|---|---|---|---|
| $\rho_0$ (fm$^{-3}$) | 0.1788 | 0.1562 | 0.1718 | 0.1813 |
| $E/A(\rho_0)$ (MeV) | −15.17 | −13.47 | −14.8 | −15.7 |
| $K$ (MeV) | 188 | 171 | 245 | 329 |
| $\Sigma_S(\rho_0,k=k_F)$ (MeV) | −368.1 | −342.1 | −404.7 | −436.3 |
| $\Sigma_0(\rho_0,k=k_F)$ (MeV) | 291.0 | 274.1 | 325.8 | 350.7 |

## III. RESULTS FOR NUCLEAR MATTER AND FINITE NUCLEI

We start from the Lagrangian given by Eq. (1). This Lagrangian is considered as an effective one with the scalar mass $m_\sigma$ and the $g_\sigma$ and $g_\omega$ coupling constants, the values of $b$, $c$, $d$, $e$, and $f$ being treated as effective parameters of our theory (although actually our approach contains only five adjustable parameters; see below).

### A. Nuclear matter

Using the RHF approach, we determine the effective parameters of our models by reproducing the DBHF nuclear matter results [equilibrium density $\rho_0$, binding energy per particle $(E/A)(\rho_0)$, compressibility modulus $K$, scalar $\Sigma_S(\rho_0,k=k_F)$, and timelike $\Sigma_0(\rho_0,k=k_F)$ components of the nucleon self-energy] obtained by a number of authors on the basis of free $NN$ forces.

We utilize here the DBHF nuclear matter results of Brockmann and Machleidt [20] obtained for different fits of one-boson-exchange potentials (we consider two versions of calculations denoted as BM-A and BM-B), and those of de Jong and Malfliet [21] (denoted as DJM and DJM-C) (see Table I). We follow the notation utilized in Ref. [24] (one can find a more detailed description of the potentials and notations in Refs. [20, 21, 24]). In the calculations we have used $M=939$ MeV, $m_\sigma=550$ MeV (or 571 MeV), $m_\omega=782.6$ MeV (or 784 MeV), $m_\rho=764$ MeV, $m_\pi=139$ MeV, $g_\pi^2/4\pi=14.81$, $g_\rho^2/4\pi=0.55$, $f_\rho/g_\rho=3.7$, and $f_\omega/g_\omega=0$. The quantities in parentheses are used in models fitting the DJM and DJM-C results.

We have performed two types of calculations with five adjustable parameters. In calculations of the first type, the values of $g_\sigma$, $g_\omega$, $b$, $c$, and $e$ or $f$ have been chosen to reproduce by our RHF calculations the DBHF nuclear matter properties, whereas $d$ was taken equal to zero. Table I gives five NM quantities corresponding to our fits in the RHF approach for each $NN$ interaction considered.

It is well known [6,7] that one-boson-exchange potentials (OBEP's) generated by the exchange of $\pi$ and $\rho$ mesons contain a repulsive contact interaction $\delta(r)$. In accordance with nonrelativistic calculations, it is possible to simulate part of the effects of short-range correlations in $\pi$ and $\rho$ contributions by removing the spurious $\delta(r)$ force from the potential part of the nuclear Hamiltonian. To see the importance of this contact interaction, we have carried out RHF calculations of infinite and finite systems considering four models specified by the following choices.

TABLE II. Adjusted parameter values of different RHF effective interactions obtained by reproducing the DBHF NM data of Table I.

| Model | $M1$ | $M2$ | $M3$ | $M4$ | $M1$ | $M2$ | $M3$ | $M4$ |
|---|---|---|---|---|---|---|---|---|
| Parameter | BM-A | | | | BM-B | | | |
| $g_\sigma^2/4\pi$ | 6.7616 | 7.6248 | 6.1715 | 7.8924 | 6.8723 | 7.9962 | 6.3821 | 8.1465 |
| $g_\omega^2/4\pi$ | 10.063 | 7.0022 | 9.0327 | 7.4593 | 10.417 | 7.6645 | 9.4424 | 7.9335 |
| $-b\times10^3$ | 5.992 | 3.904 | 7.5092 | 3.6640 | 5.381 | 3.8217 | 7.4065 | 3.6431 |
| $\overline{c}\times10^3$ | 2.828 | −5.3967 | 1.587 | −1.0646 | 4.477 | −4.933 | −0.0566 | −1.1588 |
| $\overline{e}\times10^2$ | 0 | 0 | 2.6397 | 1.9258 | 0 | 0 | 2.2598 | 1.7094 |
| $\overline{f}\times10^2$ | 2.844 | 2.1887 | 0 | 0 | 2.514 | 2.0898 | 0 | 0 |
| $e_{\rm sym}$ $(a_4)$ | 47.33 | 39.72 | 46.97 | 39.99 | 41.40 | 35.28 | 41.19 | 35.39 |
| Parameter | DJM | | | | DJM-C | | | |
| $g_\sigma^2/4\pi$ | 7.7341 | 8.9074 | 7.0264 | 9.4065 | 7.2281 | 8.7937 | 7.1844 | 9.3952 |
| $g_\omega^2/4\pi$ | 11.575 | 8.6648 | 10.294 | 9.4689 | 11.317 | 8.9903 | 11.187 | 10.036 |
| $-\overline{b}\times10^3$ | 2.785 | 2.2021 | 3.8298 | 2.0909 | 1.146 | 1.2123 | 1.3436 | 1.1423 |
| $\overline{c}\times10^3$ | 3.29 | −2.516 | 1.1664 | 1.8185 | 2.485 | −1.1453 | 8.5031 | 3.0018 |
| $\overline{e}\times10^2$ | 0 | 0 | 1.547 | 1.816 | 0 | 0 | 1.8701 | 1.7357 |
| $\overline{f}\times10^2$ | 1.888 | 1.7997 | 0 | 0 | 1.339 | 1.6415 | 0 | 0 |
| $e_{\rm sym}(a_4)$ | 48.77 | 41.78 | 48.31 | 42.29 | 52.46 | 45.17 | 52.53 | 45.92 |

Model 1 ($M1$) corresponds to $\overline{e}=0$, $\overline{f}\neq0$ (no $\delta$ force in $\pi$ and $\rho$ potentials).

Model 2 ($M2$) corresponds to $\overline{e}=0$, $\overline{f}\neq0$ (with $\delta$ force in $\pi$ and $\rho$ potentials).

Model 3 ($M3$) corresponds to $\overline{e}\neq0$, $\overline{f}=0$ (no $\delta$ force in $\pi$ and $\rho$ potentials).

Model 4 ($M4$) corresponds to $\overline{e}\neq0$, $\overline{f}=0$ (with $\delta$ force in $\pi$ and $\rho$ potentials).

The values of adjusted parameters for all these cases are presented in Table II.

Calculations of the second type, allowing the parameters $\overline{e}$ and $f$ or $d$ and $f$ to be nonzero simultaneously, have been connected with the BM-B version of the OBEP. Trying to incorporate all terms of $U_{\rm NL}$ into a self-consistent procedure, we have considered four different modifications of model 2 ($M2.1$–$M2.4$). We have used only five NM observables. Thus one of the values $d$ or $\overline{e}$ was taken equal to zero while the other one was chosen small and arbitrary to check its influence. Finally, $g_\sigma$, $g_\omega$, $b$, $\overline{c}$, and $f$ were treated as adjustable parameters. The fitting procedure was realized in the same way as for calculations of the first type. The values of the parameters obtained in this case are given in Table III. Self-consistency was achieved for all parameter sets, at all densities investigated, except in the case $M2.3$, because $m_\sigma^*$ becomes zero at densities larger than $\rho_0$ and self-consistency is lost.

The results of our calculations are illustrated by Figs. 2–7. In Fig. 2(a), the binding energy per particle $E/A$ in nuclear matter is given as a function of the Fermi momentum $k_F$ for the BM-B version of the OBE potential. Dots correspond to the DBHF data obtained by Brockmann and Machleidt in Ref. [20], while curves represent our results for models $M1$–$M4$. It is seen that the $(E/A)(k_F)$ dependence is reproduced rather accurately by our calculations for a wide range of densities; our results give similar or better fits to BM-B data than the corresponding ones obtained in Ref. [24]. The difference between models $M1$–$M4$ in reproducing the $E/A$ density dependence becomes important at relatively high densities ($k_F>1.8$ fm$^{-1}$).

In Fig. 2(b) we present the same results as in Fig. 2(a) coming from models $M2.1$, $M2$, and $M2.2$ (in all these cases the $\sigma\omega^2$ term is excluded), while in Fig. 2(c) the same results are given for models $M2.3$, $M2$, and $M2.4$ (the $\sigma^2\omega^2$ term excluded). We see that the $\sigma\omega^2$ term does not influence essentially the $(E/A)(k_F)$ dependence for NM, but the absence of the $\sigma^2\omega^2$ term may produce a drastic effect (no convergence for $M2.3$ at $k_F>1.5$ fm$^{-1}$ is achieved).

Figure 3 illustrates the $E/A$ density dependence of neutron matter [the notation being the same as in Fig. 2(a)]. Differences between models with and without $\delta(r)$ interac-

TABLE III. Same as in Table II, for the BM-B version of the OBEP, but choosing $d$ or $\overline{e}$ different of zero.

| | Model | | | |
|---|---|---|---|---|
| Parameter | $M2.1$ | $M2.2$ | $M2.3$ | $M2.4$ |
| $g_\sigma^2/4\pi$ | 10.423 | 8.4439 | 6.6306 | 11.445 |
| $g_\omega^2/4\pi$ | 10.94 | 8.3902 | 5.6006 | 13.313 |
| $-b\times10^3$ | 4.65 | 3.59 | 0.61 | 8.93 |
| $-\overline{c}\times10^3$ | 1.53 | 0.96 | 6.4 | 6.25 |
| $d$ | 0 | 0 | −0.005 | 0.005 |
| $\overline{e}$ | −0.01 | 0.01 | 0 | 0 |
| $\overline{f}$ | 0.1037 | 0.0230 | 0.041 | 0.0171 |
| $e_{\rm sym}(a_4)$ | 36.83 | 35.58 | 34.29 | 37.27 |

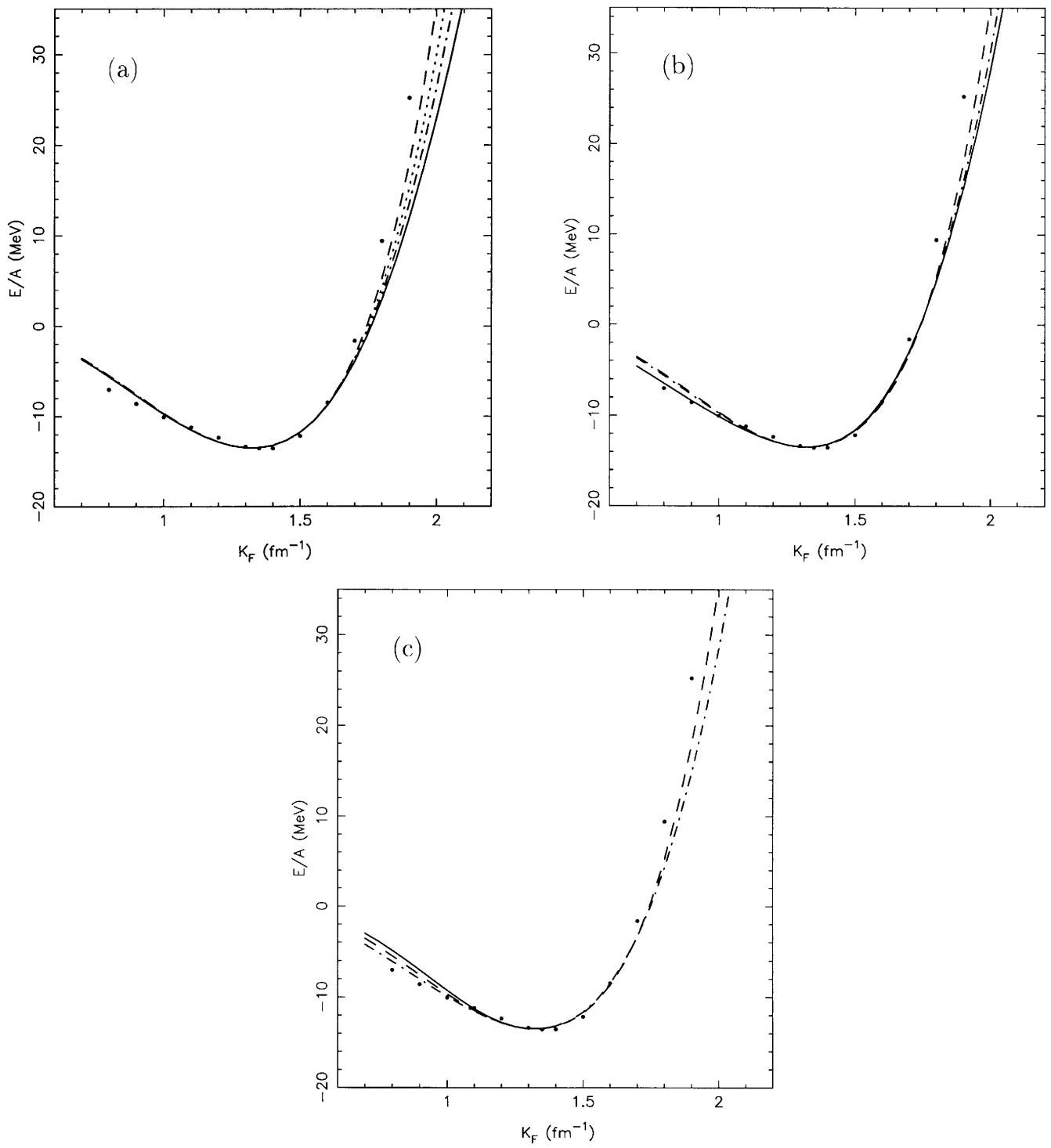


FIG. 2. (a) Binding energy per particle $E/A$ in NM as a function of Fermi momentum $k_F$ for the BM-B version of the OBE potential. The dots show the DBHF data obtained in Ref. [20]. The curves represent our results: The solid line corresponds to model $M1$, the dashed line to model $M2$, the dot-dashed line to model $M3$, and the dotted line to model $M4$. (b) The same results as in (a) but obtained for models $M2.1$, $M2$, and $M2.2$. The solid line corresponds to model $M2.1$, the dashed line to model $M2$, and the dot-dashed line to model $M2.2$. (c) The same results as in (a) but obtained for models $M2.3$, $M2$, and $M2.4$. The solid line corresponds to model $M2.3$, the dashed line to model $M2$, and the dot-dashed line to model $M2.4$.

tion in the range of nuclear densities can be explained because of the different symmetry energy values.

Contributions of separate nonlinear components of $H_1$ to the NM binding energy $E/A$ at different densities are shown in Figs. 4(a)–4(d) for models $M1-M4$, respectively, and in Fig. 4(e) for model $M2.1$, corresponding to the BM-B version of the OBE potential. One can see from these figures that the $\sigma^3$ contribution to $E/A$, for all models considered, is negative at all densities, and the contribution of the $\omega^4$ and $\sigma^2\omega^2$ terms is positive (unless these terms are included si-

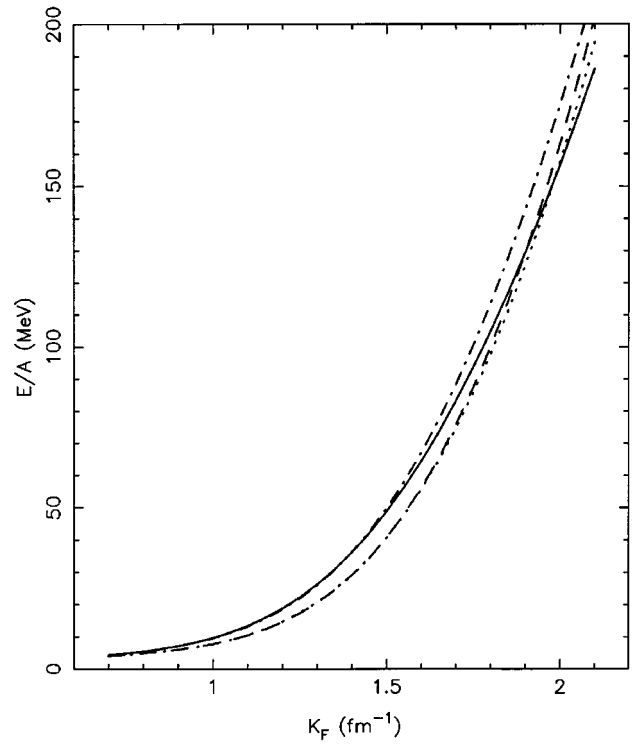


FIG. 3. The same curves and notations as in Fig. 2(a) but for neutron matter.

multaneously), while that of the $\sigma^4$ term may be negative [BM-B(1)] or positive [BM-B(2,3,4,2.1)].

In Fig. 5 we show the RHF fitting of $\Sigma_0(k_F, k=k_F)$ and $\Sigma_S(k_F, k=k_F)$ to the DBHF calculations of Ref. [20] for $M1-M4$ models corresponding to the BM-B version of the OBE potential. Our results of the spacelike component $\Sigma_V(k_F, k=k_F)$ of the nucleon self-energy are also presented (the DBHF results for this component are not available at present).

It was mentioned above that dressing of isoscalar mesons in the nuclear medium is an essential point of our approach. For this reason, the density dependence of the effective meson masses $m_\sigma^*$ and $m_\omega^*$ is shown in Figs. 6(a), 6(b), 7(a), and 7(b) for models $M2.1-M2.4$, respectively, corresponding to the BM-B potential. It should be noted that, in the case $M2.3$, $m_\sigma^*$ goes to zero at $k_F \sim 1.5$ fm$^{-1}$, almost at normal nuclear density.

An interesting NM observable is the symmetry energy ($e_{\rm sym}\alpha^2$, $\alpha$ being the asymmetry parameter). The value of $e_{\rm sym}$ at the saturation density $a_4$ has been calculated for all models considered here, and the results are shown in Tables II and III. It is seen that the BM-B potential, for models with $\delta(r)$ interaction, gives quite reasonable values of the symmetry energy coefficient, in contrast to the other versions of the OBE potentials, which give too strong values (note that $e_{\rm sym}$ is an increasing function of $\rho$ [45] and that the estimated experimental $a_4$ value is $\simeq$35 MeV [31])

The symmetry energy was obtained in all models considered here at the fixed values of $g_\rho^2/4\pi$ (=0.55) and $f_\rho/g_\rho$ (=3.7). It is worth noting that a smaller $e_{\rm sym}$ could be obtained by decreasing the $g_\rho$ value, with only very small modifications of NM properties. For instance, taking $g_\rho^2/4\pi \simeq 0.4$, as in Refs. [20, 21], the $a_4$ value is reduced about 7%.

### B. Finite nuclei

Using different sets of parameters given by Table II, we have carried out RHF calculations for the finite nuclei $^{16}$O and $^{40}$Ca. The results, including proton binding energies, total binding energies per particle (without c.m. corrections), and rms charge radii, are presented in Tables IV and V (the experimental values are given in Table VI). Models $M1$ and $M3$ [without a $\delta(r)$ interaction in $\pi$ and $\rho$ meson contributions] give appreciably more bound single-particle levels and nuclei than models $M2$ and $M4$ [with a $\delta(r)$ interaction].

These results are related to the fact that models with a repulsive $\delta(r)$ interaction need a stronger attractive finite-range force to reproduce the saturation conditions of NM. In atomic nuclei, the finite-range force is less effective than the zero-range force because of the nuclear surface. As a result, models with a repulsive $\delta(r)$ force are less bound than models without it.

The experimental binding energies for $^{16}$O and $^{40}$Ca lie between the corresponding results for models with and without a $\delta(r)$ interaction. This is what we will expect if we introduce form factors (FF's) to take care of the finite size of nucleons and take into account short-range correlation effects. Thus, because of the FF's, the repulsive $\delta(r)$ interaction is replaced by a repulsive short-range interaction and correlations do not eliminate completely this contribution.

The charge radius is too small, mainly in $M1$ and $M3$ models, which are more bound. We must note at this point that the repulsive $\delta(r)$ interaction decreases the density oscillations inside nuclei [7] and contributes to increase the charge radius.

The NM saturation density $\rho_0$ and the scalar mass $m_\sigma$ are two very important quantities in determining the charge radius. The $\rho_0$ values taken in the present paper from models BM-A, DJM, and DJM-C, are larger than the values usually used in phenomenological relativistic models [6,7] (not related to the BHF approximation). As for the bare scalar meson mass, the values of $m_\sigma$ (550 or 571 MeV) used in models BM-A, BM-B, DJM, and DJM-C are larger than the optimum ones used in phenomenological relativistic approaches to obtain a good description of finite nuclei geometrical properties [6,7]. Just these two parameters are mainly responsible for the small values of the charge radii found in this work in comparison with the experimental data. The value of the $K$ modulus, rather small in models BM-A and BM-B, is also responsible for a larger compression of nuclei because of the surface tension.

The spin-orbit splittings are too large in models giving the smallest values of the charge radii. In these cases the nuclear surface is sharper and the fields are stronger, and as a result, the spin-orbit interaction is larger.

The best models correspond to the BM-B OBEP interaction. Different choices for $d$, $e$, and $f$ have been tried. Our calculations (see Table III) show that the $d$ parameter should be very small and reasonable results can also be obtained with negative or positive small values of $e$.

In Table VI the most reasonable results of the present RHF calculation, obtained for the model $M2.1$, are compared

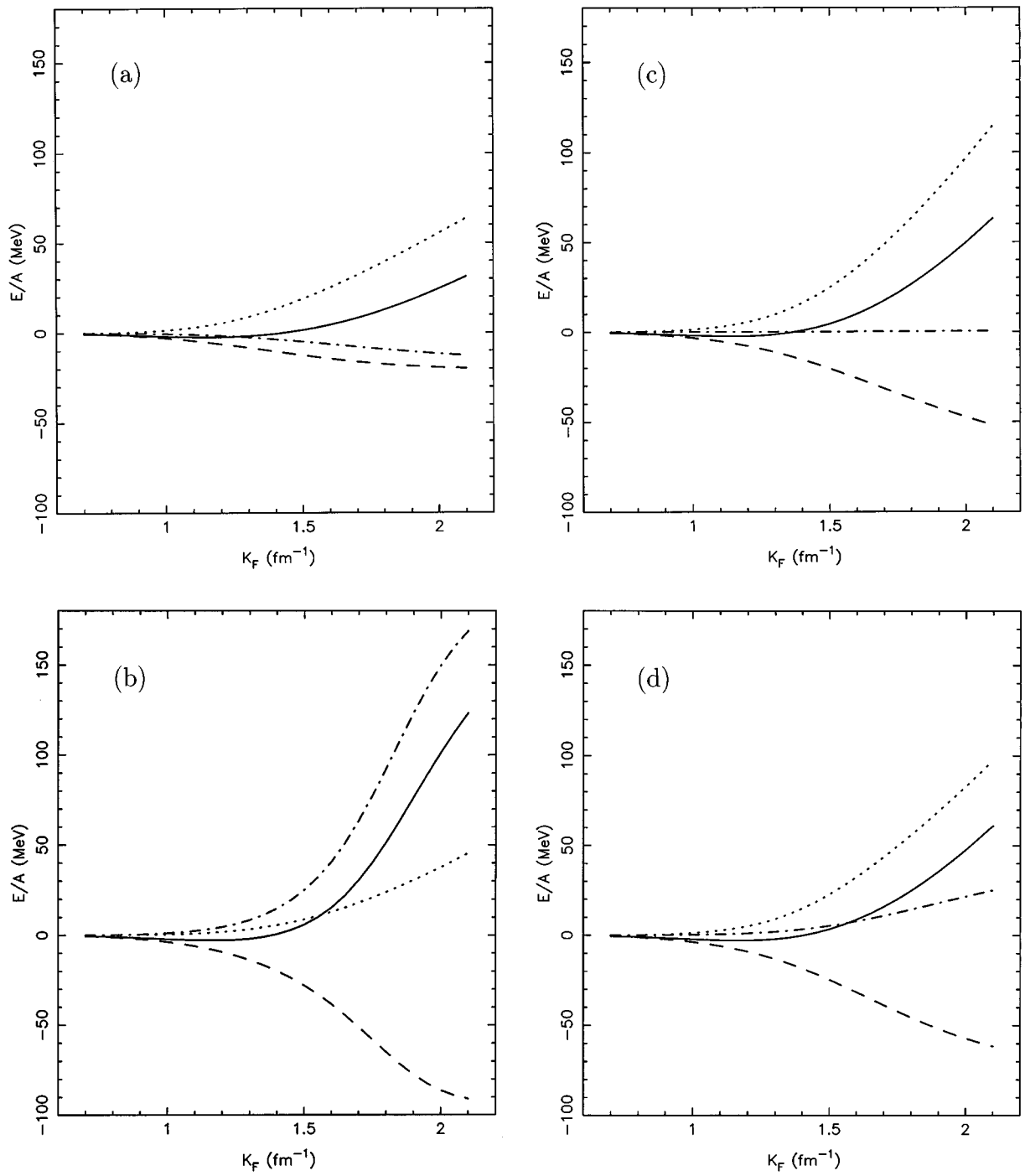


FIG. 4. (a) Contributions to the $E/A$ of separate nonlinear components of $H_1$ as functions of $k_F$ for the BM-B version of the OBE potential. Model $M1$. The dashed line corresponds to the $\sigma^3$ contribution, the dashed-dotted line to the $\sigma^4$ self-interaction, the dotted line to the $\omega^4$ term, and the solid line to the $(\sigma^3+\sigma^4+\omega^4)$ interaction. (b) The same as in (a). Model $M2$. (c) The same as in (a). Model $M3$. The dashed line corresponds to the $\sigma^3$ contribution, the dashed-dotted line to the $\sigma^4$ self-interaction, the dotted line to the $\sigma^2\omega^2$ term, and the solid line to the $(\sigma^3+\sigma^4+\sigma^2\omega^2)$ interaction. (d) The same as in (a). Model $M4$. (e) The same as in (a). Model $M2.1$. The dashed line corresponds to the $\sigma^3$ contribution, the dashed-dotted line to the $\sigma^4$ self-interaction, the dotted line to the $\sigma^2\omega^2$ term, the dashed-triple-dotted line to the $\omega^4$ self-interaction, and the solid line to the $(\sigma^3+\sigma^4+\omega^4+\sigma^2\omega^2)$ contribution.

with both the best results from Ref. [24], obtained in the RMF approximation, and the experimental data. The present calculations and those of Ref. [24], based on the BM-B interaction, contain the same number (5) of parameters: $g_\sigma$, $g_\omega$, $b$, $c$, and $f$. In $M2.1$ the $e$ value $(=-0.01)$ is chosen arbitrarily, i.e., not fitted. A detailed comparison of single-particle levels, $E/A$, $R_{\rm ch}$, and $\Delta E_{LS}$ shows that these two calculations give very close results and are in reasonable agreement with experiment.

The results for the model $M2.2$ are very similar to those of the models $M2.1$ and $M2$, although for the model $M2.1$ the nuclei are a little less bound [see $E/A(k_F)$ in Fig. 2(b)].

The problem of inverted position of levels $2s_{1/2}$-$1d_{3/2}$ obtained in Ref. [24] is also present in our calculations. Com-

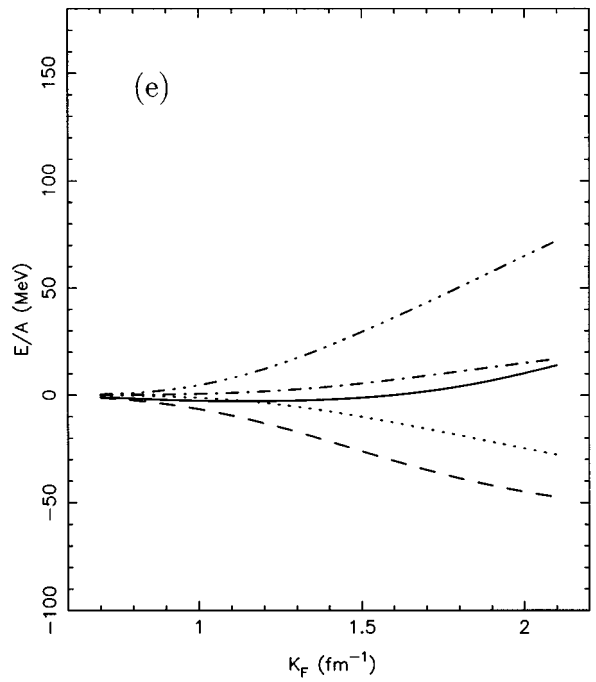


FIG. 4 (*Continued*).

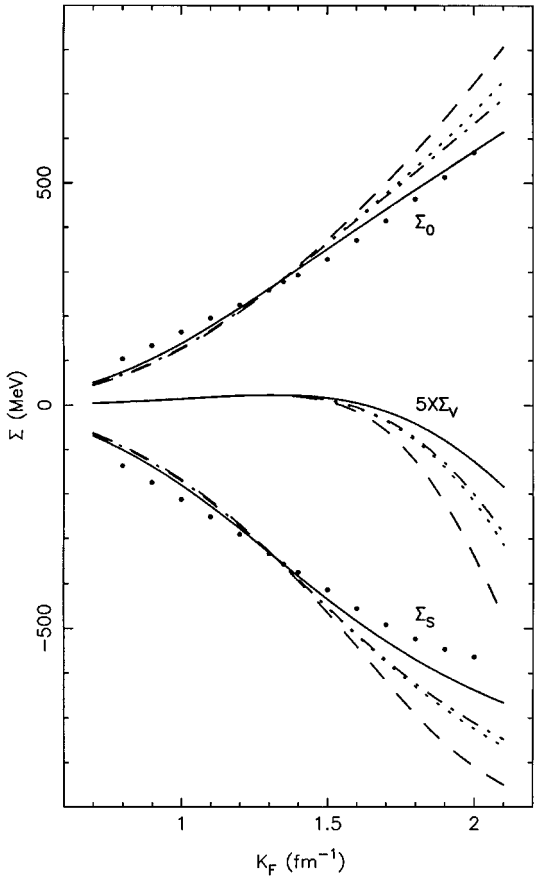


FIG. 5. Present calculations of $\Sigma_0(k_F, k=k_F)$, $\Sigma_S(k_F, k=k_F)$, and $\Sigma_V(k_F, k=k_F)$ components and for the BM-B version of the OBE potential for models $M1$–$M4$. The types of the lines are the same as in Fig. 2(a). The dots show the results for $\Sigma_0(k_F, k=k_F)$ and $\Sigma_S(k_F, k=k_F)$ from Ref. [20].

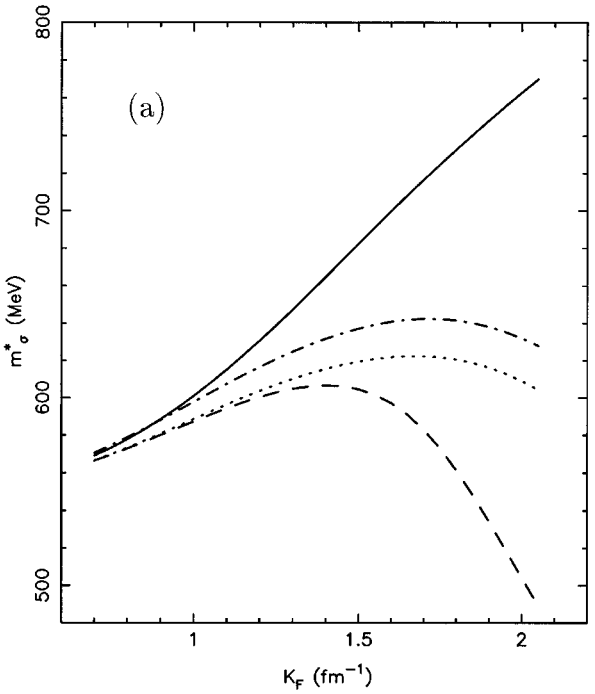


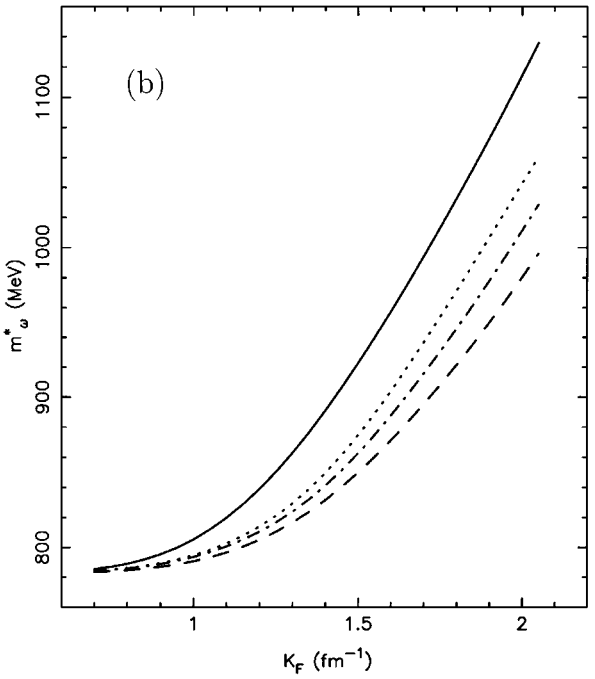


FIG. 6. (a) $m_\sigma^*$ as a function of the Fermi momentum $k_F$. The results are given for the BM-B version of the OBE potential for models $M1$–$M4$. The type of the lines are the same as in Fig. 2(a). (b) $m_\omega^*$ as a function of the Fermi momentum $k_F$. The types of the lines are the same as in Fig. 2(a).

paring the results for models $M1$ and $M3$, one can see that in absence of a $\delta(r)$ interaction in $\pi$ and $\rho$ potentials and for sets with a moderate $K$ modulus, a positive $e$ value favors a larger binding energy of the $2s_{1/2}$ level, recovering the normal single-particle order.

The saturation properties of nuclear matter $[\rho_0, E/A(\rho_0)]$ of the BM-A and DJM-C interactions are in better agreement with the usually accepted ones than those derived from BM-B and DJM interactions. On the other hand, for finite

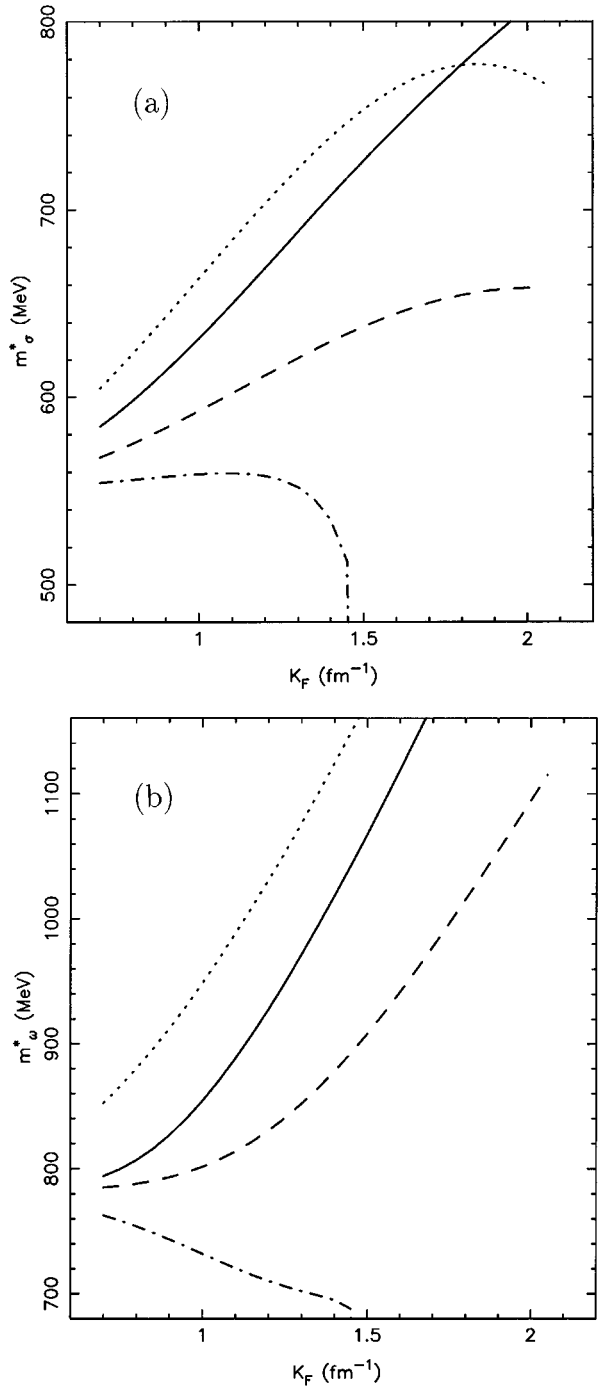


FIG. 7. (a) The same as in Fig. 6(a) but for models $M2.1$, $M2.2$, $M2.3$, and $M2.4$. The solid line corresponds to model $M2.1$, the dashed line to model $M2.2$, the dot-dashed line to model $M2.3$, and the dotted line to model $M2.4$. (b) The same as in (a) but for $m^*_\omega$.

nuclei, models based on the BM-B interaction, especially set $M2.1$, are the best ones. This observation, a little surprising, can also be extracted from the Gmuca results.

As we said before, a relatively small value of $\rho_0$, in comparison with the usually accepted one, seems to be required in RHF calculations [6,7]. On the other hand, the small value of the NM binding energy per particle in models BM-B is compensated by relatively large $m_\sigma$ and small $K$ values, which are responsible for a small surface energy in finite nuclei. This compensation is more than enough for models without $\delta(r)$ in $\pi$ and $\rho$ interactions ($M1$ and $M3$), whereas for the other models ($M2$ and $M4$) it is not enough. We would like to note down here that our calculations coincide in this point with the Gmuca results obtained in the RMF approximation [24] for the BM-B potential.

TABLE IV. Results of RHF calculations for finite nuclei for models $M1$ and $M2$.

| Model $M1$ | BM-A | BM-B | DJM | DJM-C |
|---|---|---|---|---|
| | | $^{16}$O | | |
| $1s_{1/2}$ (MeV) | 68.87 | 59.16 | 66.65 | 68.42 |
| $1p_{3/2}$ (MeV) | 35.17 | 29.30 | 35.15 | 36.96 |
| $1p_{1/2}$ (MeV) | 21.34 | 18.01 | 20.13 | 20.23 |
| $E/A$ (MeV) | 11.9 | 10.1 | 11.3 | 11.2 |
| $R_{\rm ch}$ (fm) | 2.19 | 2.31 | 2.25 | 2.24 |
| | | $^{40}$Ca | | |
| $1d_{5/2}$ (MeV) | 25.54 | 20.9 | 26.34 | 28.68 |
| $2s_{1/2}$ (MeV) | 19.78 | 14.2 | 18.26 | 16.71 |
| $1d_{3/2}$ (MeV) | 15.14 | 12.2 | 14.85 | 15.37 |
| $E/A$ (MeV) | 10.8 | 9.2 | 10.3 | 10.3 |
| $R_{\rm ch}$ (fm) | 2.95 | 3.11 | 3.01 | 2.98 |

| Model $M2$ | BM-A | BM-B | DJM | DJM-C |
|---|---|---|---|---|
| | | $^{16}$O | | |
| $1s_{1/2}$ (MeV) | 51.5 | 43.7 | 53.0 | 54.3 |
| $1p_{3/2}$ (MeV) | 23.3 | 19.5 | 25.0 | 26.1 |
| $1p_{1/2}$ (MeV) | 13.5 | 12.0 | 13.3 | 13.5 |
| $E/A$ (MeV) | 7.55 | 6.77 | 7.45 | 7.38 |
| $R_{\rm ch}$ (fm) | 2.46 | 2.59 | 2.46 | 2.45 |
| | | $^{40}$Ca | | |
| $1d_{5/2}$ (MeV) | | 16.0 | 20.9 | 22.4 |
| $2s_{1/2}$ (MeV) | | 8.99 | 8.80 | 8.54 |
| $1d_{3/2}$ (MeV) | | 8.15 | 9.19 | 9.7 |
| $E/A$ (MeV) | | 7.34 | 8.10 | 8.23 |
| $R_{\rm ch}$ (fm) | | 3.30 | 3.17 | 3.15 |

In Table VI our results are also compared to the RHF results of Ref. [30], based on the model RDHF3C and on the BM-A version of the OBE potential. The $\pi$ and $\rho$ mesons are treated similarly to the present case. The essential point of the model RDHF3C is the density dependence of the isoscalar coupling constants $g_\sigma$ and $g_\omega$. The meson-meson interactions are not taken into account. It is seen that our effective interaction approach gives a better description of single-particle spectra, binding energies, and, especially, spin-orbit splittings than the approximation considered in Ref. [30].

## IV. SUMMARY

In the present paper we have investigated various types of effective interactions calculating the ground-state properties of finite nuclei in the relativistic framework. As mentioned above, an investigation of the same type is carried out by

TABLE V. Results of RHF calculations for finite nuclei for models $M3$ and $M4$.

| Model $M3$ | BM-A | BM-B | DJM | DJM-C |
|---|---|---|---|---|
| | $^{16}$O | | | |
| $1s_{1/2}$ (MeV) | 74.5 | 65.6 | 71.7 | 68.8 |
| $1p_{3/2}$ (MeV) | 38.8 | 33.2 | 38.7 | 37.3 |
| $1p_{1/2}$ (MeV) | 21.7 | 18.5 | 20.3 | 20.2 |
| $E/A$ (MeV) | 10.4 | 9.9 | 11.0 | 11.2 |
| $R_{\rm ch}$ (fm) | 2.14 | 2.24 | 2.20 | 2.24 |
| | $^{40}$Ca | | | |
| $1d_{5/2}$ (MeV) | 27.2 | 22.4 | 28.0 | 28.9 |
| $2s_{1/2}$ (MeV) | 29.2 | 27.5 | 25.6 | 17.3 |
| $1d_{3/2}$ (MeV) | 15.7 | 12.9 | 14.8 | 15.4 |
| $E/A$ (MeV) | 10.7 | 9.12 | 10.1 | 10.3 |
| $R_{\rm ch}$ (fm) | 2.90 | 3.03 | 2.96 | 2.98 |
| Model $M4$ | BM-A | BM-B | DJM | DJM-C |
| | $^{16}$O | | | |
| $1s_{1/2}$ (MeV) | 45.4 | 42.8 | 50.8 | 53.0 |
| $1p_{3/2}$ (MeV) | 20.2 | 19.2 | 24.0 | 25.6 |
| $1p_{1/2}$ (MeV) | 12.5 | 12.0 | 13.6 | 13.9 |
| $E/A$ (MeV) | 6.80 | 6.82 | 7.68 | 7.60 |
| $R_{\rm ch}$ (fm) | 2.55 | 2.61 | 2.49 | 2.46 |
| | $^{40}$Ca | | | |
| $1d_{5/2}$ (MeV) | 16.73 | 15.6 | 20.1 | 21.9 |
| $2s_{1/2}$ (MeV) | 9.24 | 8.68 | 8.39 | 8.27 |
| $1d_{3/2}$ (MeV) | 8.47 | 8.13 | 9.65 | 9.98 |
| $E/A$ (MeV) | 7.47 | 7.39 | 8.28 | 8.38 |
| $R_{\rm ch}$ (fm) | 3.24 | 3.33 | 3.21 | 3.17 |

Gmuca in Ref. [24]. In both cases the effective interactions are derived from the same DBHF results. However, these two effective approaches differ in the general structure of the effective interaction and in the presence (or absence) of the Fock-exchange terms.

We aim to provide a direct link between the nucleon-nucleon interaction and the nuclear structure within a relativistic model, taking into account all reasonable mesons $\sigma$, $\omega$, $\pi$, and $\rho$ (both vector and tensor couplings). The effective interaction just contains the nonlinear functional $U_{\rm NL}$ of the most simple general form compatible with relativistic invariance requirements, including all possible terms of interaction and self-interactions of isoscalar meson fields of order not higher than quartic in meson fields.

In Ref. [24], the RMF approach was adopted and, consequently, the contributions of $\pi$ and $\rho$ mesons were ignored. Furthermore, only self-interactions of the $\sigma$ and $\omega$ meson fields were involved, the $\sigma\omega^2$ and $\sigma^2\omega^2$ terms being completely ignored.

Our approach contains five fitting parameters, just the same number as in Ref. [24], which have been adjusted by reproducing within the RHF method the DBHF data for NM. The two remaining parameters have been chosen in an arbitrary way.

TABLE VI. Present calculations are compared with the relativistic mean-field results obtained in Ref. [24] (BM-B version of the OBE potential), the relativistic HF results of Ref. [30] (designated as RDHF3C), and the experimental data. The calculations of Ref. [30] include $\pi$ and $\rho$ mesons and are based on the BM-A version of the OBEP.

| | Present theory | BM-B version of Ref. [24] | Ref. [30] | Experiment [43,44] |
|---|---|---|---|---|
| | $^{16}$O | | | |
| $s_{1/2}$ (MeV) | 43.7 | 41.07 | 42.98 | $40\pm8$ |
| $p_{3/2}$ (MeV) | 20.0 | 18.77 | 21.31 | 18.4 |
| $p_{1/2}$ (MeV) | 13.2 | 12.38 | 15.72 | 12.1 |
| $\Delta E_{p_{1/2-3/2}}$ (MeV) | 6.8 | 6.39 | 5.59 | 6.3 |
| $-E/A$ (MeV) | 7.81 | 7.89 | 7.41 | 7.98 |
| $R_{\rm ch}$ (fm) | 2.59 | 2.53 | 2.68 | 2.73 |
| | $^{40}$Ca | | | |
| $d_{5/2}$ (MeV) | 15.91 | 14.54 | 18.95 | 15.5 |
| $2s_{1/2}$ (MeV) | 7.41 | 6.92 | 13.78 | 10.9 |
| $d_{3/2}$ (MeV) | 8.99 | 8.66 | 12.67 | 8.3 |
| $\Delta E_{d_{3/2-5/2}}$ (MeV) | 6.92 | 5.88 | 6.28 | 7.2 |
| $-E/A$ (MeV) | 8.09 | 7.72 | 7.81 | 8.55 |
| $R_{\rm ch}$ (fm) | 3.35 | 3.38 | 3.35 | 3.48 |

Our results show that the $\sigma\omega^2$ term does not influence essentially the NM binding energy density dependence, while the contribution of all other components of $U_{\rm NL}$ is much more important.

Models connected with the BM-B potential, especially those without a $\delta(r)$ force, give very good values of the symmetry energy. The Fock terms play an important role in determining this quantity. Note that the RMF approximation considered in Ref. [24] (without a $\rho$ meson) gives $a_4$ values close to 20 MeV.

The effective interaction obtained is utilized to calculate finite nuclei properties (see Tables IV–VI), without introducing new additional parameters.

To make a direct comparison with the RMF results of Ref. [24], our calculations are restricted to the same nuclei $^{16}$O and $^{40}$Ca which were considered by Gmuca. The results shown in Tables IV and V, obtained using the effective Lagrangian without either $\sigma^2\omega^2$ or $\omega^4$ terms, for all models considered and all versions of OBE potentials are rather poor in comparison with experiments and previous studies [6,7]. However, the results given in Table VI (model $M2.1$, based on the BM-B version of the OBEP), obtained when both $\sigma^2\omega^2$ and $\omega^4$ terms are included, look quite reasonable. This fact shows that $\sigma^2\omega^2$ and $\omega^4$ terms of $U_{\rm NL}$ are essential components of the effective Lagrangian adopted here; moreover, as seen from Table III, the negative value of the coefficient $\overline{e}$ (determining the strength of the $\sigma^2\omega^2$ interaction) is preferable ($\overline{e}=-0.01$). The important role of the $\sigma^2\omega^2$ term is demonstrated also by calculations in the model $M2.3$. Convergence is lost when this term is neglected.

The approach developed here can be considered as a method avoiding complete DBHF calculations for finite structures. Inclusion of self-interactions and interactions between different meson fields leads to meson dressing, i.e., to the density dependence of the meson effective masses. Meson dressing in the nuclear medium is one of the key ingredients of our theory. Thus the effective interaction introduced in this paper may be considered as a convenient tool to investigate the influence of the medium effects on the meson propagators in calculating properties of nuclear structures within the RHF framework.

## ACKNOWLEDGMENTS

Two of the authors (L.N.S. and V.N.F.) are very grateful to the University of Cantabria for hospitality. All of the authors are also very thankful to Nguyen Van Giai for helpful discussions.

[1] J. D. Walecka, Ann. Phys. (N.Y.) **83**, 491 (1974); B. D. Serot and J. D. Walecka, in *Advances in Nuclear Physics*, edited by J. W. Negele and E. Vogt (Plenum, New York, 1986), Vol. 16, p. 1.
[2] G. E. Brown, W. Weise, G. Baym, and J. Speth, Comments Nucl. Part. Phys. **17**, 39 (1987).
[3] N. V. Giai and L. N. Savushkin, Fiz. Elem. Chastits At. Yadra **23**, 847 (1992); Sov. J. Part. Nucl. **23**, 373 (1992).
[4] A. Bouyssy, S. Marcos, and Pham Van Thieu, Nucl. Phys. **A422**, 541 (1984).
[5] M. Rufa, P.-G. Reinhard, J. A. Maruhn, W. Greiner, and M. R. Strayer, Phys. Rev. C **38**, 390 (1988).
[6] A. Bouyssy, J. F. Mathiot, N. V. Giai, and S. Marcos, Phys. Rev. C **36**, 380 (1987).
[7] P. Bernardos, V. N. Fomenko, N. V. Giai, M. López-Quelle, S. Marcos, R. Niembro, and L. N. Savushkin, Phys. Rev. C **48**, 2665 (1993).
[8] V. N. Fomenko, L. N. Savushkin, S. Marcos, R. Niembro, and M. López-Quelle, J. Phys. G **21**, 53 (1995); Yad. Fiz. **58**, 258 (1995) [Phys. At. Nuclei **58**, 214 (1995)].
[9] M. R. Anastasio, L. S. Celenza, W. S. Pong, and C. M. Shakin, Phys. Rep. **100**, 327 (1983).
[10] R. Brockmann and R. Machleidt, Phys. Lett. **149B**, 283 (1984).
[11] B. ter Haar and R. Malfliet, Phys. Rep. **149**, 207 (1987).
[12] R. Machleidt, K. Holinde, and Ch. Elster, Phys. Rep. **149**, 1 (1987).
[13] R. Machleidt, in *Advances in Nuclear Physics*, edited by J. W. Negele and E. Vogt (Plenum, New York, 1989), Vol. 19, p. 189.
[14] R. Malfliet, in *Progress in Particle and Nuclear Physics*, edited by A. Faessler (Pergamon, Oxford, 1988), Vol. 21, p. 207.
[15] H. Müther, R. Machleidt, and R. Brockmann, Phys. Lett. B **202**, 483 (1988).
[16] L. S. Celenza, Shun-fu Gao, and C. M. Shakin, Phys. Rev. C **41**, 1768 (1990); H. B. Ai, L. S. Celenza, A. Harindranath, and C. M. Shakin, *ibid.* **35**, 2299 (1987); H. B. Ai, L. S. Celenza, and C. M. Shakin, *ibid.* **39**, 236 (1989).
[17] H. Elsenhans, H. Müther, and R. Machleidt, Nucl. Phys. **A515**, 715 (1990).
[18] S. Marcos, R. Niembro, M. López-Quelle, N. V. Giai, and R. Malfliet, Phys. Rev. C **39**, 1134 (1989).
[19] S. Marcos, M. López-Quelle, and N. V. Giai, Phys. Lett. B **257**, 5 (1991).
[20] R. Brockmann and R. Machleidt, Phys. Rev. C **42**, 1965 (1990).
[21] F. de Jong and R. Malfliet, Phys. Rev. C **44**, 998 (1991).
[22] H. Müther, R. Machleidt, and R. Brockmann, Phys. Rev. C **42**, 1981 (1990).
[23] R. Brockmann and H. Toki Phys. Rev. Lett. **68**, 3408 (1992).
[24] S. Gmuca, Nucl. Phys. **A547**, 447 (1992); J. Phys. G **17**, 1115 (1991); Z. Phys. A **342**, 387 (1992).
[25] R. Fritz, H. Müther, and R. Machleidt, Phys. Rev. Lett. **71**, 46 (1993).
[26] R. Fritz and H. Müther, Phys. Rev. C **49**, 633 (1994).
[27] S. Haddad and M. K. Weigel, Phys. Rev. C **48**, 2740 (1993).
[28] H. F. Boersma and R. Malfliet, Phys. Rev. C **49**, 233 (1994).
[29] H. F. Boersma and R. Malfliet, Phys. Rev. C **49**, 1495 (1994).
[30] Hua-lin Shi, Bao-qiu Chen, and Zhong-yu Ma, Phys. Rev. C **52**, 144 (1995).
[31] R. J. Furnstalhl, B. D. Serot, and Hua-Bin Tang, Nucl. Phys. **A598**, 539 (1996).
[32] S. A. Moszkowski and C. G. Kallman, Nucl. Phys. **A287**, 495 (1977).
[33] J. Boguta and A. R. Bodmer, Nucl. Phys. **A292**, 413 (1977).
[34] J. Boguta, Nucl. Phys. **A372**, 386 (1981).
[35] J. Boguta and S. A. Moszkowski, Nucl. Phys. **A403**, 445 (1983).
[36] J. Boguta and H. Stocker, Nucl. Phys. **B120**, 289 (1983).
[37] W. Pannert, P. Ring, and J. Boguta, Phys. Rev. Lett. **59**, 2420 (1987); Y. K. Gambhir and P. Ring, Phys. Lett. B **202**, 5 (1985).
[38] K. Sumiyoshi, D. Hirata, H. Toki, and H. Sagawa, Nucl. Phys. **A552**, 437 (1993).
[39] A. R. Bodmer and C. E. Price, Nucl. Phys. **A505**, 123 (1989); A. R. Bodmer, *ibid.* **A526**, 703 (1991).
[40] E. K. Heide, S. Rudaz, and P. J. Ellis, Nucl. Phys. **A571**, 713 (1994).
[41] K. Sumiyoshi, H. Kuwabara, and H. Toki, Nucl. Phys. **A581**, 725 (1995).
[42] H. Kouno, K. Koide, T. Mitsumori, N. Noda, and A. Hasegawa, Phys. Rev. C **52**, 135 (1995).
[43] X. Campi and D. W. L. Sprung, Nucl. Phys. **A194**, 401 (1972).
[44] H. de Vries, C. W. de Jager, and C. de Vries, At. Data Nucl. Data Tables **36**, 495 (1987).
[45] M. L. Quelle, S. Marcos, R. Niembro, A. Bouyssy, and N. Van Giai, Nucl. Phys. **A483**, 479 (1988).